JOURNAL OF APPLIED POLYMER SCIENCE VOL. 17, PP. 2203-2212 (1973)

Mechanism of Yield and Fracture in ABS Materials

EDWARD M. HAGERMAN, *General Motors Research Laboratories, Warren, Michigan 48090*

Synopsis

Four commercial grades of ABS of varying physicomechanical properties were fractured in tension at three straining rates. Photomicrographs of the fracture surfaces were used to qualitatively describe the effects of straining rate on craze growth. Based on a micrograph of what is assumed to be the first stress-activated state of craze formation, a model describing the function of the elastomer phase in these materials is presented.

INTRODUCTION

Acrylonitrile–butadiene–styrene (ABS) terpolymers have been shown to be two-phased in nature with the styrene–acrylonitrile (SAN) components comprising a continuous matrix. Interspersed in this matrix, the polybutadiene exists as spherical inclusions.[1,2,3] The overall system may be described as a rigid matrix containing numerous low-modulus, elastomeric inclusions. The mechanical properties of these materials may be varied from the high-modulus (5×10^5 psi), brittle (5% elongation at break) SAN copolymer on the one hand to low-modulus (2.4×10^5), ductile (80% elongation) ABS, through the introduction of the proper elastomer. Furthermore, properties intermediate between these extremes are obtainable, and indeed numerous grades and types of ABS are commercially available.

The mechanism by which ABS absorbs energy has been the subject of numerous papers beginning with the Mertz et al. theory[4] describing the elastomer phase acting as rubber bands holding the newly formed fracture surfaces together. More recent papers tend to fall into either of two categories. The craze theorists, beginning with Bucknall and Smith,[5] propose that the elastomer particles act as stress concentration sites and under the influence of applied load numerous crazes are generated and propagated. Crazes or stress whitening may be defined as flat, reflecting dislocations formed at right angles to the applied stress and consisting of 40% to 60% void and 60% to 40% highly oriented matrix material.[6] In order to be operable, the craze theory requires only the presence of numerous stress concentration sites generating numerous crazes without formation and propagation of major cracks.

Another theory, proposed by Newman and Strella,[7] suggests that the elastomer acting under triaxial stress initiates a dilation of the matrix

TABLE I
Mechanical Properties of ABS and SAN Materials

Material designation	Tensile strength, psi	Tensile modulus, psi	Elongation at break at 5 in./min, %	Izod impact, ft lb/in.
A (ABS)	4,800	2.4×10^5	94	7.7
B (ABS)	5,900	3.0×10^5	38	6.5
C (ABS)	6,000	3.1×10^5	30	7.0
D (ABS)	6,500	3.4×10^5	46	5.5
SAN	11,000	5.0×10^5	2.5	0.4

structure and allows drawing to occur in the vicinity of the elastomer particles. The energy-absorbing mechanism is then the drawing of the rigid matrix. In a later paper,[8] Strella presented a mathematical expression relating the degree of expected cubical dilation in terms of the physicomechanical properties of the matrix and dispersed-phase materials. The equation predicts that maximum impact enhancement would result from both the matrix and elastomer phase moduli tending to zero. This prediction has been confirmed experimentally.[9]

In attempting to rationalize these two mechanisms, it became apparent that the craze theory did not predict the effect of varying the modulus of the elastomeric inclusion, requiring only that the elastomer be above its glass transition temperature at the testing conditions. The matrix drawing theory, on the other hand, did not predict the existence of crazes which certainly are associated with ABS fracture. These discrepancies between fact and theory would seem to indicate that the true sequence of events leading to fracture in ABS has not yet been fully defined.

EXPERIMENTAL

Our experimental procedure was to fracture ASTM type-S tensile bars in a simple tension test. Photomicrographs of the fracture surfaces were made using the Jelco scanning beam electron microscope. Magnifications used were generally 60× to detect gross variations in the overall fracture surface and 10,000× to observe the fine detail of the fracture event.

Since such factors as elastomer concentration and physicomechanical properties[9,10] are known to affect the impact strength, elongation, tensile strength, and modulus, it was decided to use four different grades (Table I) of ABS and look for gradations in the photomicrographs. Furthermore, since both of the current theories of ABS fracture require polymer flow, either in the matrix or the craze matter, the tensile tests were performed at three different straining rates. Since polymer flow is strain-rate dependent, testing at 5, 400, and 4000 in./min should show any rate effects in the fracture detail. All tests were carried out at room temperature on injection-molded specimens. The 5 in./min tests were done on an Instron machine, while the 400 in./min and 4000 in./min tests required the Plastechon Model 581 tester. At least three samples of each material were broken at each test rate. All samples were gold coated and were observed under the electron microscope. The photographs presented are representative of the given material at the given straining rate. The sample orientation in the microscope was such that the view was approximately looking straight down on the plane of fracture.

INTERPRETATION OF THE MICROGRAPHS

The 60× micrographs revealed little concerning the actual mechanism of fracture (Fig. 1). The site of fracture initiation is plainly visible and varied from edge defects to flaws within the material bulk. Material A,

the most ductile (highest elongation, lowest modulus), showed evidence of massive drawing occurring even as the fracture was propagating. In the other samples, the 60× micrographs showed a relatively planar fracture surface with occasional hyperbolic markings resulting from main fracture

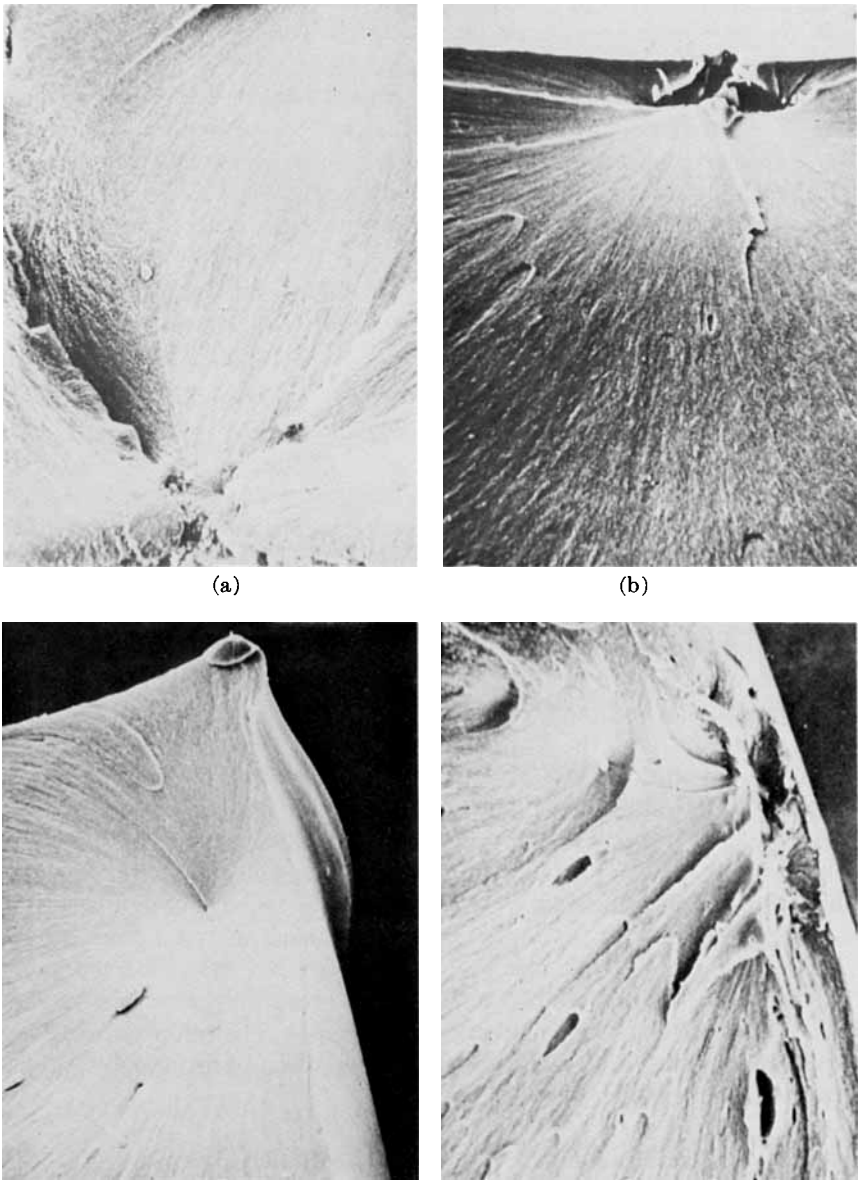

(a) (b)

(c) (d)

Fig. 1. Photomicrographs of ABS fracture surfaces. Magnification 60×, test rate 4000 in/min. (a) Material A; (b) material B; (c) material C; (d) material D.

Fig. 2. Fracture surface micrograph of material D. Magnification 10,000×, test rate 5 in./min.

activation of secondary flaws along the fracture path. As a whole, this series of micrographs showed that fracture initiates at naturally occurring flaws which are randomly distributed throughout the bulk of the material.

The 10,000× micrographs showed substantially more detail which could be attributable to the actual mechanism of the energy absorption process. Figure 2 shows a 10,000× magnification of the surface of material D obtained at 5 in./min straining rate. The micrograph clearly shows the highly drawn, fibrillar structure of the crazed surface. Assuming the fracture to have proceeded through the center of the craze field, the thickness of the craze band at failure was approximately 4 microns. A surprising feature of this micrograph was the complete lack of any evidence of the elastomeric inclusion. The elastomer particle size has been estimated to be in the range of 2–10 microns in diameter.[3,7] If present, particles of this diameter should be readily visible. This suggests that crazes are associated with the ultimate failure of these materials, but the response may be homogeneous rather than multiphased in nature.

DISCUSSION

Associated with the ultimate fracture of any material will be a critical value of the stress. We have shown that ABS fracture initiation takes place at a flaw in the molded part. Such flaws are known to be sites of stress concentration. In addition, polymers because of their randomly kinked and folded chain structure have the facility to unfold and thus

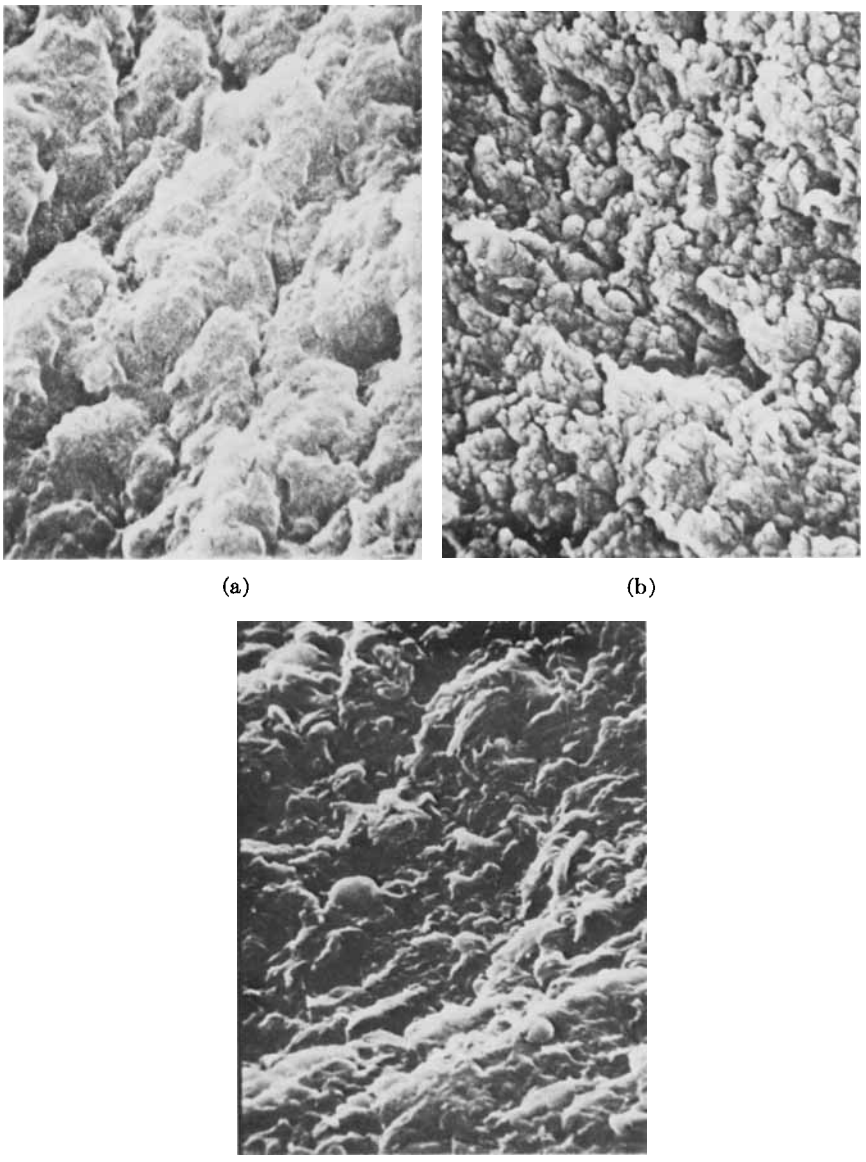

Fig. 3. Fracture surface micrograph of material A. Magnification 10,000×. (a) rate, 4000 in./min; (b) rate, 400 in./min; (c) rate, 5 in./min.

relieve applied stress. Such stress relaxation processes are time dependent in that finite times are required for this unfolding to occur. In the first approximation, then, the critical fracture stress is achieved from the applied load times some stress concentration factor, appropriate to the flaw at the fracture initiation site, less any stress lost to relaxation processes. Figure 3 shows material A fractured at 4000, 400, and 5 in./min straining rates.

Magnification used was 10,000× in each case. The micrographs show the craze structure associated with the fracture of the same material under varying conditions of straining rate. The same critical value of stress must have been attained in each case, however, at lower elongations in samples tested at the higher straining rates. Figure 3b can be viewed as a continuation of drawing initiated in the 3a structure. Figure 3c represents a continuation of 3b; however, heat generated in the drawing of the overall sample and the locally high elongation at the craze was sufficient to melt the craze matter and allow the craze field to collapse. This occurred only in the most ductile material, tested at the lowest straining rate. Again, no evidence of any features on the 2–10 micron range relatable to the elastomer particles could be found. Viewed as a series, Figure 3 shows the fracture response of the material as its stress relaxation capacities are being reduced by fracturing at rates faster than the uncoiling and unfolding responses to stress can occur. Interpreted from another perspective, the fracture was occurring earlier and earlier during the craze growth process. The fracture of the other ABS materials tested in this series could be interpreted as above, with the thickest crazes being generated at the lower straining rates and lower-modulus materials generating thicker craze layers than higher-modulus materials. Such results would be expected from a critical stress criteria for fracture of the craze layer.

Material D (highest modulus) (Fig. 4) provided substantially more information on the craze initiation step. Micrograph 4a shows the well-developed craze field associated with low-rate fracturing. Craze thickness, approximately twice the observed, would be around 4 microns. In 4b, fractured at 400 in./min, the average craze thickness was approximately 2 microns at fracture. In 4c, fractured at 4000 in./min, a true craze field has not yet been generated. This micrograph shows what must be the very first step in the establishment of a craze layer. This layer does not possess the fibril-like structure of the true craze but instead a uniform distribution of spherical voids of about 0.2 micron in diameter. Such voids were noted by Kambour[11] in his study of the craze phenomena in polycarbonate. In that study, spherical voids were noted at the extreme tip of the craze with craze thickening, i.e., fibril formation, occurring only at some distance from the craze tip proper. Furthermore, void formation has been associated with ductile fracture of copper.[12] Indeed, the description of the copper fracture process would in general describe craze formation in polymers. Void formation at stress concentration sites in numerous ductile metals has been similarly described in the literature.[13]

Void formation thus appears to be a general response of ductile materials to the locally high stresses at stress concentration sites. Analysis of the stress fields associated with effective stress concentrators, such as notches, etc., have shown that a state of almost pure hydrostatic tension[14] exists in small volumes of material at the flaw/bulk material interface. It is the nature of these triaxial fields that no displacements are possible. That is, since the incremental volume of material is being pulled equally in all

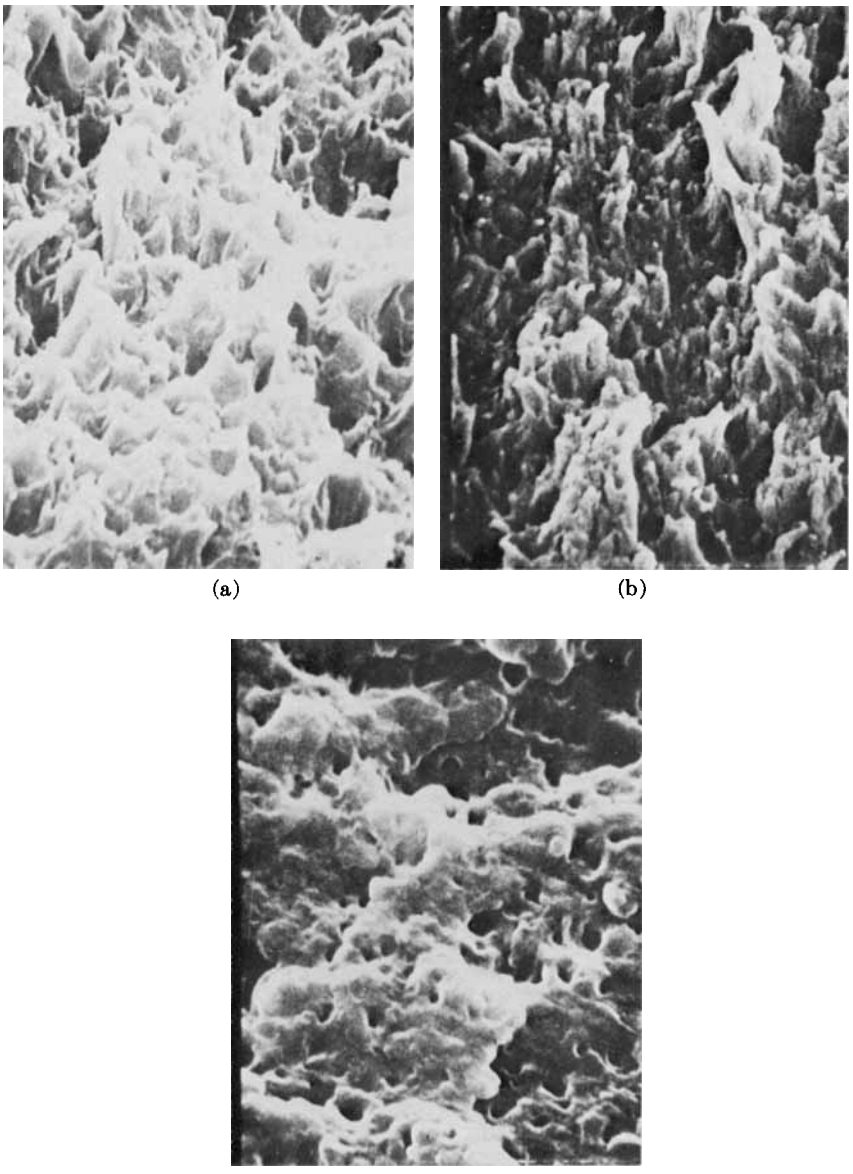

Fig. 4. Fracture surface micrograph of material D. Magnification 10,000×. (a) rate, 5 in./min; (b) rate, 400 in./min; (c) rate, 4000 in./min.

directions, no motion is possible. Since the stress relaxation processes imply molecular movement, such relaxations are not possible unless the triaxial state of stress is in some way dissipated. It appears that void formation is the mechanism by which such triaxial stresses are relieved. Such a sequence of events implies that the initial stress activated state is the

formation of a layer of material containing voids and as such the newly formed layer is incapable of sustaining a triaxial state of stress. Following void formation, large displacements are possible and drawing into fibrils follows. The nature of the stress-induced molecular dilation necessary to explain the drawing process has been described by Litt and Tobolsky.[15]

CONCLUSIONS

The micrographs show that, most certainly, crazing is a feature of the fracture process of ABS. Equally important is the lack of any evidence of the elastomer particles associated with the craze field at fracture. From this it could be concluded that the ABS fracture response is much like any of the many[16] homogeneous polymers which fail via the craze mechanism. How, then, is the brittle SAN transformed into the ductile ABS by adding spherical particles of elastomer?

A very simple model describing this behavior may be suggested, based on Figure 4c and Kambour's work with polycarbonate.[11] The elastomer particles of specified size, shape, distribution, and properties act to approximate the void-containing layer shown in 4c. The model differs from previous models[4,5,7] in that the influence of the individual particles is not considered important. The important feature is the array of particles whose modulus approaches zero. The means by which the stress vector in the thickness (Z-axis) direction is minimized may be viewed as follows. Firstly, it is well known that thick plates are more susceptible to brittle fracture than thin plates. Izod impact results, normalized to 1 in. notch width, are always lower for $^1/_2$-in. cross-section samples than for $^1/_8$-in. cross-section specimen of the same material. This is attributable to the increasing triaxiality of the stress field with thicker samples. The Z-axis stresses are developed from Poisson's ratio effects, and the magnitude of these stresses is a function of the specimen thickness. We may view the elastomer particles acting to interfere with the generation of these internal stresses. The effective thickness for generation of the Z-axis stress in ABS may be considered to be the distance between elastomeric inclusions. The requirement for lowest possible modulus in the elastomer phase may be explained from the point of view that the lower the modulus the smaller the amount of stress which could be transferred across the inclusion and therefore the lower overall Z-axis stress. The effect of increasing elastomer content is to simply reduce the distance between elastomer particles and lower still further the Z-axis stress.

Assuming this model, the entire bulk of the ABS material would, in the unstressed state, duplicate SAN under a state of stress very near fracture. The initial response to stress of such a model would be homogeneous drawing of the entire stressed mass. Such a response would readily explain the 50% reduction in modulus between SAN and the sample A material. The sequence of events leading to fracture is as follows: The entire bulk of the material begins homogeneous yielding very early in the loading history; at

some level of strain, a critical stress is achieved at a stress concentration site, voids are generated, and craze growth begins. As straining continues, fracture proceeds along the craze line. Energy is consumed in the homogeneous plastic deformation and in the craze-growth steps, with sufficient heat generated to melt the material, under the proper circumstances.

Such a model would tend to generalize the fracture mechanisms of ABS and of such amorphous, homogeneous materials as polycarbonate. Indeed, generalizations could be drawn between certain ductile fractures in metals such as copper and in polymers.

The author wishes to thank Mr. T. P. Schreiber of GMR Analytical Chemistry Department for the preparation of the electron photomicrographs.

References

1. R. Buchdahl and L. E. Nielsen, *J. Polym. Sci.*, **15**, 1 (1955).
2. K. Durges and H. Schuster, *Makromol. Chem.*, **101**, 200 (1967).
3. K. Kato, *Polym. Eng. Sci.*, **7**, 38 (1967).
4. E. H. Mertz, G. C. Claver, and M. J. Baer, *J. Polym. Sci. A-1*, **4**, 1595 (1966).
5. C. B. Bucknall and R. R. Smith, *Polymer*, **6**(8), 437 (1965).
6. R. P. Kambour, *Polymer*, **5**(3), 143 (1967).
7. S. Newman and S. Strella, *J. Appl. Polym. Sci.*, **9**, 2297 (1965).
8. S. Strella, *J. Polym. Sci. A-2*, **4**, 527 (1966).
9. E. M. Hagerman, *J. Appl. Polym. Sci.*, **13**, 1873 (1969).
10. C. H. Basdekis, *ABS Plastics*, Reinhold, New York, 1964, p. 36.
11. R. P. Kambour, *Polymer*, **5**, 143 (1964).
12. H. C. Rogers, *Trans. Metallur. Soc. AIME*, **218**, 504 (1960).
13. T. Yokobori, *An Interdisciplinary Approach to Fracture and Strength of Solids*, Walters-Noordhoff Scientific Publications, Groningen, 1968, p. 171.
14. *Ibid.*, p. 182.
15. M. Litt and A. V. Tobolsky, *J. Macromol. Sci., Phys. B-1*, **3**, 587 (1967).
16. R. P. Kambour, *J. Polym. Sci. A-2*, **4**, 17 (1966).

Received December 7, 1972